Melittin-Lipid Bilayer Interactions and the Role of Cholesterol

Per Wessman,* Adam A. Strömstedt,† Martin Malmsten,† and Katarina Edwards*
*Department of Physical and Analytical Chemistry, and †Department of Pharmacy, Uppsala University, Uppsala, Sweden

ABSTRACT The membrane-destabilizing effect of the peptide melittin on phosphatidylcholine membranes is modulated by the presence of cholesterol. This investigation shows that inclusion of 40 mol % cholesterol in 1-palmitoyl-2-oleoyl-*sn*-glycero-3-phosphocholine or 1,2-dioleoyl-*sn*-glycero-3-phosphocholine liposomes reduces melittin's affinity for the membrane. It is significant that the presence of cholesterol does not increase the amount of membrane-associated melittin needed to cause maximum leakage from, or major structural rearrangements of, the liposomes. Furthermore, comparison of microscopy and leakage data suggests that melittin-induced leakage occurs via different mechanisms in the cholesterol-free and cholesterol-supplemented systems. In the absence of cholesterol, leakage of carboxyfluorescein takes place from intact liposomes in a manner compatible with the presence of small melittin-induced pores. In the presence of cholesterol, on the other hand, adsorption of the peptide causes complete membrane disruption and the formation of long-lived open-bilayer structures. Moreover, in the case of cholesterol-supplemented systems, melittin induces pronounced liposome aggregation. Cryotransmission electron microscopy was used, together with ellipsometry, circular dichroism, turbidity, and leakage measurements, to investigate the effects of melittin on phosphatidylcholine membranes in the absence and presence of cholesterol. The melittin partitioning behavior in the membrane systems was estimated by means of steady-state fluorescence spectroscopy measurements.

INTRODUCTION

The bee venom peptide melittin has been studied extensively due to its lytic effects on biological and model membranes (1,2). Although the natural target for melittin is eukaryotic membranes (3) and the peptide is too cytotoxic to be used as an antibiotic, melittin is an interesting model peptide. It shares important features with other antimicrobial peptides, e.g., the magainins and cecropins (4), and belongs to the group of membrane-perturbing peptides that are amphiphilic and cationic and adopt a more or less pronounced linear α-helical conformation when bound to bilayer interfaces (5). More specifically, melittin is composed of 26 amino acids, of which residues 1–20 are predominantly hydrophobic, whereas residues 21–26 are hydrophilic. Four of the six positive charges are located in the latter region (1,2). At low concentrations, melittin exists as a monomer in aqueous solution, but it self-associates at concentrations $>\sim 100$ μM to form tetramers (6,7). Due to its amphiphatic character, melittin readily associates with other amphiphilic structures such as lipid bilayers. A more detailed overview of the properties of the peptide can be found in reviews by, e.g., Dempsey (2), and Raghuraman and Chattopadhyay (1).

Numerous studies have addressed different aspects of the membrane-perturbing effect of melittin. The general picture, obtained largely from studies based on release of liposome-entrapped low-molecular-weight dyes, is that melittin induces membrane leakage at comparably low peptide/lipid mixing ratios (R_i). Several mechanisms, including the formation of well-defined membrane pores, as well as more diffuse lipid packing defects, have been proposed to explain the increase in membrane permeability. Although the influence on lipid composition has not been fully elucidated, and there exist some seemingly conflicting experimental observations (8,9), melittin is believed to permeabilize the membrane by inducing the formation of distinct membrane pores. Moreover, data from several studies (10–12) support a mechanism whereby melittin at a critical peptide/lipid ratio promotes the establishment of toroidal pores in the membrane (13). Cholesterol is well known to have a pronounced reducing effect on melittin-induced leakage from phosphatidylcholine (PC) lipid membranes (14). It has been suggested that the apparently better resistance of cholesterol-containing membranes to permeabilization is a consequence of cholesterol's membrane-condensing effect, which precludes deep melittin penetration (3,14). Indeed, recent studies have confirmed that melittin penetrates deeper into pure dioleoylphosphatidylcholine (DOPC) bilayers compared to DOPC bilayers supplemented with >20 mol % cholesterol (15). At high R_i, larger-scale membrane perturbations and eventually solubilization into small peptide/lipid mixed micelles take place. For gel-phase PC membranes, fragmentation of the bilayers into discrete discoidal structures with diameters in the range 200–400 Å has been observed at submicellization concentrations of peptide (16–19). NMR studies indicate an inhibitory effect of cholesterol on the disc-formation process (20,21). No disc formation has so far been verified in pure PC systems at temperatures above the lipid gel-to-liquid crystalline phase transition temperature.

Despite the large number of studies published, the relation between the small-scale perturbations causing leakage at low peptide/lipid ratios and the more pronounced bilayer rearrangements eventually leading to micellization has not yet

Submitted January 31, 2008, and accepted for publication July 10, 2008.

Address reprint requests to Per Wessman, Uppsala University, Dept. of Physical and Analytical Chemistry, Box 579, Uppsala 751 23, Sweden. Tel: 46-707-310718; E-mail: per.wessmen@fki.uu.se.

Editor: Thomas J. McIntosh.

0006-3495/08/11/4324/13 $2.00

doi: 10.1529/biophysj.108.130559

been thoroughly investigated. In a recent report, we indicated that melittin-induced morphological changes of the bilayer other than pore formation are partly responsible for the leakage observed from DOPC/cholesterol liposomes at low peptide/lipid molar ratios (22). In this study, we have extended our research to include cholesterol-supplemented palmitoyloleoylphosphatidylcholine (POPC) membranes, as well as pure DOPC and POPC membranes. An important aim of the investigation was to correlate and compare the amount of bilayer-associated melittin needed in the different systems to induce significant liposome leakage and major structural rearrangements. Because interpretation and comparison of data required knowledge about the effective peptide/lipid ratio in the membrane, we used a fluorescence-based technique to investigate the partition behavior of melittin in the four different lipid systems.

MATERIAL AND METHODS

Materials

POPC (1-palmitoyl-2-oleoyl-*sn*-glycero-3-phosphocholine) and DOPC (1,2-dioleoyl-*sn*-glycero-3-phosphocholine) were from Avanti Polar Lipids (Alabaster, AL). Cholesterol, *n*-dodecyl β-D-maltoside (DDM) 98+% pure, and NaCl, Na_2HPO_4, NaH_2PO_4, and melittin ≥95% pure (determined by HPLC) were obtained from Sigma Aldrich Chemical (Steinheim, Germany). Melittin was dissolved in phosphate-buffered saline (PBS), 10 mM phosphate 150 mM NaCl pH 7.3, with an osmolality of 295 mmol/kg. Melittin solutions of 30 μM were then frozen immediately after preparation and kept at –20°C until used. 5(6)-Carboxyfluorescein (CF) was from Molecular Probes (Leiden, The Netherlands), and aqueous stock solutions of 100 mM CF were prepared in saline-free phosphate buffer. The solution, isoosmolar with the PBS, was adjusted to pH 7.3. All reagents and salts were used as received.

Liposome preparation

Lipid mixtures were prepared by dissolving the lipids in $CHCl_3$, then removing the solvent under a gentle stream of nitrogen gas and evaporating the remaining $CHCl_3$ in vacuum. After drying, the lipid films were hydrated in either PBS or, in the case of leakage experiments, saline-free CF solution. The lipid mixtures were then subjected to five freeze-thaw cycles and subsequently extruded 30 times through two polycarbonate filters of pore size 100 nm using a Lipo-Fast extruder (Avestin, Ottawa, Canada). Untrapped CF buffer was separated from the liposomes by gel filtration over a PD-10 desalting column from Amersham Biosciences (Uppsala, Sweden). It has been shown that bilayers formed from DOPC and DOPC/cholesterol under certain conditions have a tendency to transform into inverted structures (23,24). However, as judged from cryotransmission electron microscopy (cryo-TEM), the freshly prepared liposome samples used in these experiments did not contain any such structures.

Turbidity measurements

Optical density measurements were carried out at 25°C on melittin-lipid mixtures. The lipid concentrations were 1 mM for the DOPC and POPC systems and 2 mM for the DOPC/cholesterol and POPC/cholesterol systems. An HP 8453 absorbance spectrophotometer (Hewlett Packard, Böblingen, Germany) was used at a wavelength of 350 nm.

Partition studies

The partitioning of melittin between the aqueous and bilayer phases was estimated by taking advantage of the fact that the fluorescence emission spectra of the single tryptophan residue in melittin shifts to shorter wavelengths when the peptide partitions into lipid membranes. This blue shift arises due to the less polar environment experienced by the tryptophan residue in the lipid membrane (25). The steady-state fluorescence measurements were performed at 25°C with a SPEX Fluorolog 1650 0.22-m double spectrometer (SPEX Industries, Edison, NJ), using an excitation wavelength of 280 nm and acquiring emission spectra between 320 and 365 nm. During each experiment, aliquots of a 10-mM liposome suspension were added to an aqueous melittin solution, and emission spectra were acquired after each addition. The shift was quantified by taking the ratio of the intensities acquired at 325 and 355 nm, respectively, corrected for inner filter effects (25). The magnitude of the shift was used to determine the fraction, α, of melittin that had partitioned into the lipid membranes, and was followed as a function of the peptide/lipid molar mixing ratio, R_i. Association isotherms describing the partitioning process were then constructed from the mixing ratio and the fraction of membrane-associated melittin. The isotherms were fitted to the expression (26)

$$(\alpha \times R_i)/((1-\alpha) \times [P]_{tot,aq}) = R_{eff}/[P]_{aq} = K_P/\gamma_P^{lip}, \quad (1)$$

where $[P]_{tot,aq}$ is the total aqueous concentration of melittin, R_{eff} the actual or effective peptide/lipid ratio in the membrane, $[P]_{aq}$ the actual melittin concentration in the buffer, K_P the partition coefficient (M^{-1}), and γ_P^{lip} an activity coefficient introduced to account for deviation from ideal partition behavior. We define the activity coefficient as an exponential function of R_{eff} and a parameter w that accounts for electrostatic interactions as well as changes in membrane mechanical properties due to peptide association with the membrane.

$$\gamma_P^{lip} = \exp(w \times R_{eff}). \quad (2)$$

Once K_P and w are known for a specific lipid composition, R_{eff} can be calculated for any chosen R_i by using, in combination with Eq. 2, an iterative process involving the expression

$$R_{eff} = [P]_{L,aq}/[lip]_{aq} = ([P]_{tot,aq} \times Kp)/(Kp \times [lip]_{aq} + \gamma_P^{lip}), \quad (3)$$

where $[P]_{L,aq}$ is the aqueous concentration of membrane-associated melittin and $[lip]_{aq}$ is the total aqueous concentration of lipid.

A small amount (0.25 mol %) of uncharged PEG(5000)-ceramide was included in the POPC/cholesterol samples employed in the partition studies. The reason for this was that melittin in this system induced a pronounced aggregation that was likely to interfere with the fluorescence measurements. Inclusion of the PEG-lipid counteracted this aggregation but had, at this low concentration, an insignificant effect on the binding isotherm, as confirmed by control experiments in the DOPC/cholesterol system (data not shown). Unless otherwise stated, the measurements were performed at 25°C.

Surfaces

Silica slides with an oxide-layer thickness of 30 nm (Okmetic, Espoo, Finland), were used as a bilayer-supporting substrate for the ellipsometry experiments. These slides were cleaned at 80°C for 5 min in water solutions of first 3.6% NH_4OH and 4.3% H_2O_2, then 4.6% HCl and 4.3% H_2O_2, and then kept in 99% ethanol. After use, the surfaces were cleaned by gas plasma discharges with a Harrick Plasma Cleaner PDC-32G (Harrick Plasma, Ithaca, NY) at 18 W in 0.2 Torr residual air for 5 min. The surfaces thus obtained displayed an advancing contact angle of $<10°$.

Ellipsometry

Melittin adsorption to supported lipid bilayers was studied by in situ null ellipsometry using an Optrel Multiskop ellipsometer (Optrel, Allershausen, Germany) with a 100-mW argon laser at 532 nm, and an angle of incidence of

67.66°. Measurements were carried out at 37°C in a 5-ml minimum-tension quartz cuvette under stirring (300 rpm). The adsorption was evaluated by monitoring changes in the state of polarization after reflection at the bilayer-coated silica slides. From this, the refractive index (n) and layer thickness (d) of the adsorbed layer were determined. With these parameters, the adsorbed amount (Γ) was calculated according to de Feijter et al. (27), using a refractive-index increment (dn/dc) of 0.154 cm^3/g (28,29). Corrections were routinely made to compensate for any change in bulk refractive index caused by changes in temperature or excess electrolyte concentration.

The bilayer constituents were deposited as described in detail previously (29). In short, mixed micellar solutions were prepared by dissolving the dried film in a 19-mM DDM water solution. The resulting micellar solutions were either 86 mol % DDM and 14 mol % phospholipid (DOPC or POPC) or 97.3 mol % DDM, 1.6 mol % phospholipid, and 1.1 mol % cholesterol. The solution was added to the cuvette and lipid deposition was monitored until it stabilized. Deposited DDM was then removed by rinsing with Milli-Q water (Millipore, Billerica, MA). By repeating this procedure and gradually lowering the concentration of the micellar solution, stable, densely packed bilayers are formed, with a defect density of <10%. When the bilayer formation was completed, the temperature raised from 25 to 37°C, and water exchanged for PBS, melittin was added cumulatively to concentrations of 0.025, 0.1, and, finally, 0.4 μM in the cuvette, and the adsorption was monitored. All measurements were done in duplicate.

Leakage experiments

For the leakage experiments, we used the same SPEX-fluorolog as in the partitioning studies. A HI-TECH Rapid Kinetics Accessory mixer model SFA-II (Hi-Tech Scientific, Salisbury, England) was used to bring about a rapid mixing of equal volumes of melittin solution and the liposome suspension. The excitation and emission wavelengths were set to 495 and 520 nm, respectively, and the intensity recorded at 0.1-s intervals. The lipid concentration was kept at 12 μM after mixing to keep the concentration-dependent fluorescence signal from the released CF within the linear range. The melittin concentration was between 0.10 and 1.0 μM after mixing. To determine the fluorescence intensity when all CF had leaked out, a solution of 8 mM Trition-X was mixed with the liposomes instead of melittin. The degree of leakage, expressed as the percent of total leakage, $L(t)$, was followed with time according to the relationship

$$L(t) = 100 \times ((I(t) - I_0)/(I_{tot} - I_0)), \quad (4)$$

where $I(t)$ is the time-dependent intensity increase after addition of melittin, I_0 the intensity before addition of melittin, and I_{tot} the intensity after addition of triton-X. The fluorescence signal was measured for a period of 15 min and the temperature was kept at 25°C.

Cryo-TEM studies

The cryogenic transmission microscopy investigations were performed with a Zeiss EM 902A transmission electron microscope (Carl Zeiss, Oberkochen, Germany). The instrument was operating at 80 kV and in zero-loss bright-field mode. Digital images were recorded under low-dose conditions with a BioVision Pro-SM Slow Scan CCD camera. (Proscan, Scheuring, Germany) and analySIS software (Soft Imaging System, Münster, Germany). To visualize as many details as possible, an underfocus of 1–2 μm was used to enhance the image contrast.

Briefly, the method for sample preparation was as follows, with a more comprehensive description available in Almgren et al. (30). Samples were equilibrated at 25°C and ~99% relative humidity within a climate chamber. A small drop of sample (~1 μl) was deposited on a copper grid covered with a perforated polymer film and with thin evaporated carbon layers on both sides. Excess liquid was thereafter removed by blotting with a filter paper, leaving a thin film of the solution on the grid. Immediately after blotting, the sample was vitrified in liquid ethane, held just above its freezing point. Samples were kept below –165°C and protected against atmospheric conditions during both transfer to the TEM and examination. Samples of the desired R_{eff} were prepared by mixing liposome and melittin solutions of adequate concentrations. The lipid concentrations used were 0.5–5 mM. Unless otherwise stated, all specimens were vitrified <15 min after sample preparation.

Circular dichroism measurements

The secondary structure of melittin, either free in solution or associated with liposomes, was measured by circular dichroism using a JASCO J810 spectropolarimeter (JASCO, Easton, MD). The concentrations used were 2 μM melittin and 800 μM lipid. Scanning was done through a 2-mm quartz cuvette at 20°C, between 200 and 260 nm at 50 nm/min and 30 accumulations. The α-helix content was quantified in the interval between 222 nm (31) and 225 nm (32). Monomeric poly-L-lysine was used as reference for 100% α-helix in 0.1 M NaOH and 100% random coil in 0.1 mM HCl (32). To correct for baseline drift between measurements, the background value (detected at 250–260 nm, where no peptide signal is present) was subtracted for each individual sample measurement. Signals from nonpeptide components were also corrected for and measurements were performed in triplicate.

RESULTS

Analysis of the association isotherms

For technical reasons, the turbidity, leakage, circular dichroism (CD), ellipsometry, and cryo-TEM measurements had to be performed at different lipid concentrations, and thus the size of the lipid phase varied between experiments. To correlate the results with the actual amount of melittin associated with the lipid membranes, R_{eff}, an estimate of the partitioning of melittin in the different lipid systems was needed. Fig. 1 shows the association isotherms obtained for the lipid systems with the fluorescence method. Equation 1 could be well fitted to these isotherms. The fitting parameters K_P and w, where K_P is the molar partition coefficient and w gives a measure of the extent to which the partitioning process deviates from the ideal, are collected in Table 1. As revealed in Fig. 1, the association behavior of melittin is strongly affected by variations in the lipid composition of the liposomes. The amount of peptide actually associated with the membrane at a specific peptide/lipid mixing ratio, R_i, consequently varies depending on the choice of liposome system. Results of this study indicate that the tendency for melittin to associate with the different liposome membranes decreases in the system order DOPC > POPC > DOPC/cholesterol > POPC/cholesterol.

As shown in the inset of Fig. 1, increasing the temperature from 25 to 37°C had no major effect on melittin's tendency to associate with DOPC or POPC liposome membranes. It is important to note that the order of the curves did not change, and melittin association was clearly more pronounced in the DOPC compared to the POPC system at the higher temperature as well.

Turbidity measurements

Turbidity measurements were carried out to follow major changes in size and aggregation behavior that took place upon

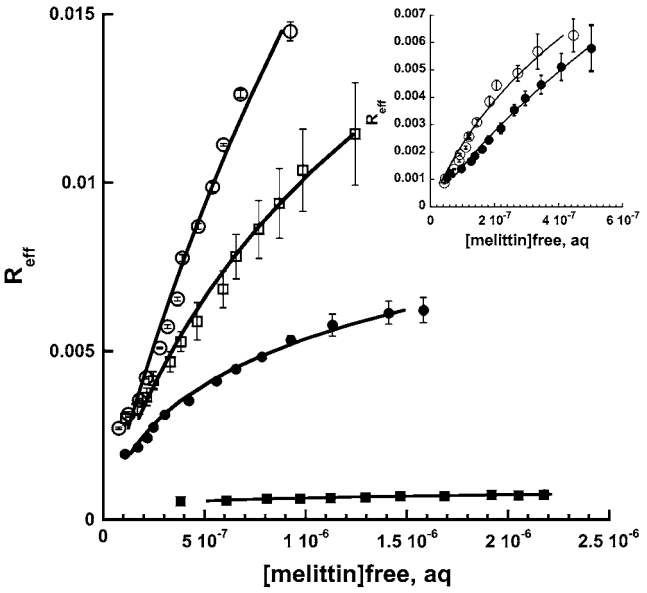

FIGURE 1 Association isotherms recorded for melittin at 25°C in systems containing DOPC (*open circles*), POPC (*open squares*), DOPC/cholesterol 60:40 (*solid circles*), and POPC/cholesterol 60:40 (*solid squares*) liposomes. R_{eff} corresponds to mol membrane-associated melittin/mol lipid; and [melittin]free, aq is the concentration of unassociated or free melittin in the aqueous phase. (*Inset*) Association isotherms for the DOPC (*open circles*) and POPC (*solid circles*) systems at 37°C.

addition of melittin to the liposome samples. As can be seen in Fig. 2, the turbidity in the pure POPC and DOPC systems was only marginally affected by the presence of melittin. In the cholesterol-containing systems, on the other hand, melittin induced a pronounced turbidity increase. It is noteworthy that in the DOPC/cholesterol system the turbidity dropped drastically at high R_{eff}. A similar behavior was noticed in the POPC/cholesterol system, too, but only after the samples had been incubated for 24 h (data not shown).

Melittin association as probed by ellipsometry

The ellipsometry measurements show the tendency for melittin to adsorb to the supported bilayers. From Fig. 3, it is clear that cholesterol reduces melittin association with both DOPC and POPC bilayers, which is in agreement with the data from the fluorescence study of melittin association with liposomal bilayers. However, the ellipsometry results indicate that the peptide associates more avidly to POPC than to DOPC bilayers. The origin of this seeming discrepancy is not yet known, but may be related to the underlying substrate affecting the POPC and DOPC membranes differently in terms of their sensitivity to melittin binding.

Helical content of bound melittin

Fig. 4 displays the fraction of melittin in α-helical conformation as determined by CD measurements in samples with 800 μM lipid concentration and $R_i = 2.5 \times 10^{-3}$. For the pure DOPC and POPC liposome systems, this mixing ratio and lipid concentration correspond to R_{eff} values (2.37×10^{-3} and 2.34×10^{-3} for DOPC and POPC, respectively), where the liposomes according to cryo-TEM investigation (see Figs. 6 and 7) remain intact and structurally unperturbed. Under the given conditions, the membrane-bound fractions of the added melittin are furthermore similar enough in the DOPC and POPC systems (95% and 94%, respectively) to allow for a direct comparison of the data presented in Fig. 4. Thus, the CD measurements suggest that melittin has a considerably higher α-helix content when associated with DOPC than when associated with POPC membranes. More specifically, the fraction of melittin in the α-helical conformation corresponds, after correction for the 20% helix content of melittin dispersed in the aqueous phase, to 88% and 55% in DOPC and POPC membranes, respectively. The latter value is in good agreement with earlier results reported by Constantinescu and Lafleur (33).

Data corrected for aqueous melittin suggest that DOPC/cholesterol and POPC/cholesterol systems have a helix content corresponding to 82% and 41%, respectively. The evaluation of the CD results obtained in the cholesterol-supplemented systems is, however, not straightforward. For technical reasons, neither the mixing ratio nor the lipid concentration could be adjusted sufficiently to ensure R_{eff} values low enough to avoid melittin-induced structural changes in the samples. Thus, the CD measurements were carried out under conditions in which the samples, according to cryo-TEM investigations (see Figs. 8 and 9), are structurally heterogeneous and contain disrupted liposomes. As discussed below, this fact complicates the interpretation of data.

TABLE 1 Fitting parameters for partitioning behavior in the four membrane systems

	K_P ($10^3 \times M^{-1}$)	w	z_P	R_i	R_{eff}
DOPC	23.4	24	1.7	2.5×10^{-2}	5.0×10^{-3}
POPC	21.1	72	2.1	8.3×10^{-3}	1.5×10^{-3}
DOPC/cholesterol	25.7	292	5.5	7.5×10^{-2}	5.0×10^{-3}
POPC/cholesterol*	27.9	5860	20	4.2×10^{-2}	5.5×10^{-4}

K_P is the molar partitioning coefficient derived from the fit of the association isotherms, w is the fitting parameter that accounts for deviation from ideal partitioning, the fitting parameter z_P is the effective charge of melittin in accordance with the Gouy-Chapman approach. R_i is the melittin/lipid mixing ratio and R_{eff} is the calculated amount of membrane-associated melittin needed to cause maximum release of liposome-entrapped carboxyfluorescein within 15 min after mixing.

*We included 0.25 mol % of the lipid ceramide-PEG(5000) in the POPC/cholesterol liposomes used for the partition study.

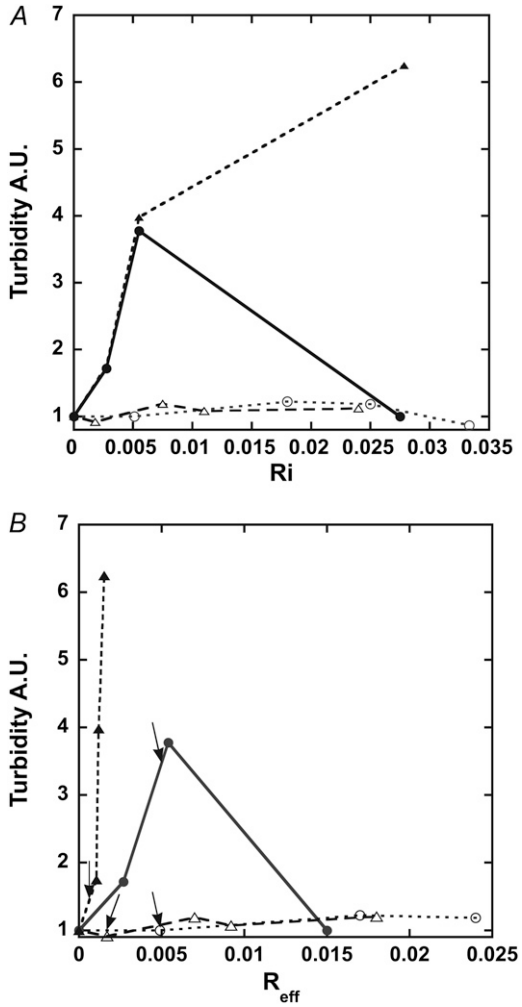

FIGURE 2 (*A*) Turbidity plotted as a function of R_i, i.e., the melittin/lipid mixing ratio for DOPC (*open circles*), POPC (*open triangles*), DOPC/cholesterol 60:40 (*solid circles*), and POPC/cholesterol 60:40 (*solid squares*). The lipid concentrations are 1 mM for DOPC and POPC and 2 mM for DOPC/cholesterol and POPC/cholesterol. (*B*) Turbidity plotted as a function of R_{eff}, i.e., mol membrane-associated melittin/mol lipid for DOPC (*open circles*), POPC (*open triangles*), DOPC/cholesterol 60:40 (*solid circles*), and POPC/cholesterol 60:40 (*solid squares*). The arrows indicate the R_{eff}s at which melittin causes maximum leakage of liposome-entrapped CF for each system (see Table 1).

Bilayer perturbations probed by leakage experiments

The effect of melittin on membrane permeability was probed by leakage experiments. Typical leakage curves are presented in Fig. 5. For all systems, the release rate was found to increase with increasing melittin concentration. It is noteworthy that whereas melittin, with time, induced total release of the CF entrapped in POPC, DOPC, and POPC/cholesterol liposomes, no more than 72% of the probe was released from liposomes composed of DOPC/cholesterol. The R_i values and R_{eff} values needed to cause maximum release of liposome-entrapped CF within 15 min after peptide addition are displayed in Table 1. For purposes of comparison, in Fig. 2, which displays the melittin-induced turbidity changes, arrows mark the R_{eff} values reported in Table 1.

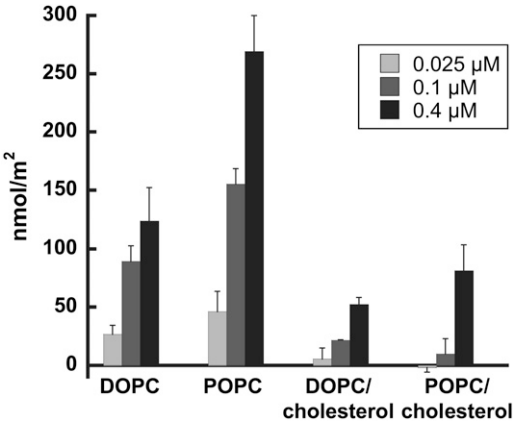

FIGURE 3 Ellipsometry data showing the equilibrium amount of melittin adsorbed to supported bilayers composed of DOPC, POPC, DOPC/cholesterol 60:40, and POPC/cholesterol 60:40. Melittin concentrations correspond to 0.025, 0.1, and 0.4 μM. Measurements were carried out in duplicate at 37°C.

Changes in the membrane morphology visualized by cryo-TEM

Cryo-TEM was employed to directly visualize melittin-induced morphological changes of the liposomes. Samples with melittin/lipid ratios corresponding to R_{eff} values below and above those needed to cause maximum leakage within 15 min (Table 1) were investigated for each of the different lipid

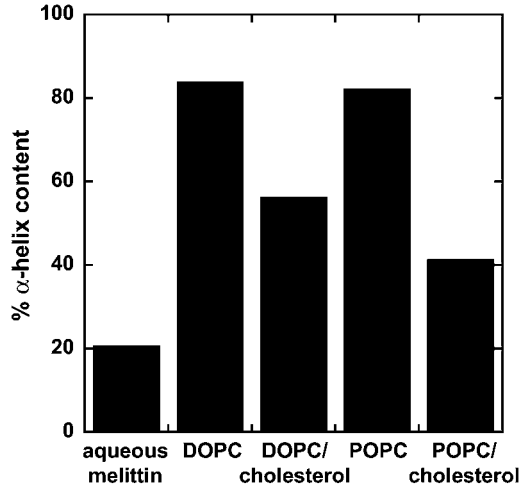

FIGURE 4 The α-helix content of melittin as probed by CD measurement in PBS buffer and in the presence of liposomes composed of either DOPC, DOPC/cholesterol 60:40, POPC, or POPC/cholesterol 60:40. The error bars show standard deviations from triplicate experiments. The concentrations used were 2 μM melittin and 800 μM lipid. Measurements were carried out at 20°C.

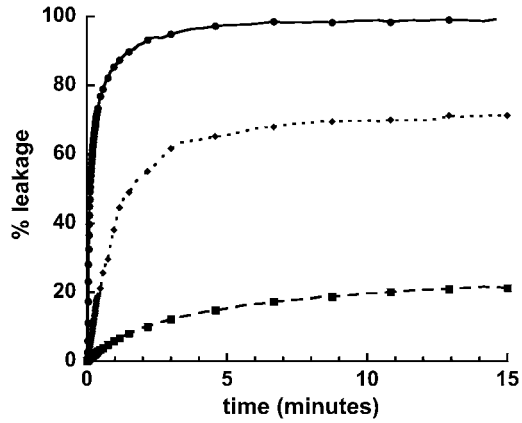

FIGURE 5 Leakage curves obtained after addition of melittin to DOPC liposomes (*solid circles*) and DOPC/cholesterol 60:40 liposomes (*solid squares*) at $R_i = 0.025$ (corresponding to $R_{eff} = 0.005$ and 0.003, respectively) and to DOPC/cholesterol liposomes (*solid diamonds*) at $R_i = 0.075$ ($R_{eff} = 0.005$).

compositions. Based on the cryo-TEM investigations, it is possible to distinguish some important differences in the effects of melittin on structural behavior in the different liposome systems.

In the pure DOPC and POPC systems (Figs. 6 and 7), the liposomes exhibited no discernible changes in size or morphology at R_{eff} values corresponding to those reported in Table 1. This implies that the melittin-induced CF leakage took place from intact liposomes. However, micrographs

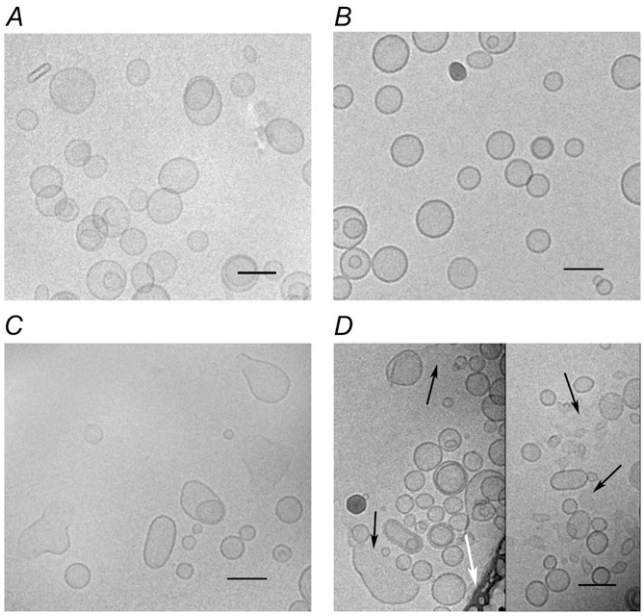

FIGURE 6 Aggregate structures as revealed by cryo-TEM before (*A*) and after (*B–D*) melittin addition to DOPC liposomes. (*B*) Liposomes at $R_{eff} = 5.0 \times 10^{-3}$ ($R_i = 5.0 \times 10^{-3}$). (*C* and *D*) Examples of structures found at $R_{eff} = 1.7 \times 10^{-2}$ (*C*) and 2.4×10^{-2} (*D*) ($R_i = 1.8 \times 10^{-2}$ and 2.7×10^{-2}, respectively). Black arrows indicate open structures and the white arrow indicates a polymer film. Scale bar, 100 nm.

obtained from samples with higher R_{eff} displayed clear signs of major structural rearrangement. In both systems, ruptured liposomes and open-bilayer structures were frequently observed in coexistence with closed liposomes (e.g., Figs. 6 *C* and 7 *C*). It is interesting that many small open-bilayer structures with a diameter of ~100 nm were found at high R_{eff} (Fig. 7 *D*). These structures were stable over time, as confirmed by reanalysis of the samples after 72 h incubation (Fig. 7 *E*).

The cryo-TEM investigations revealed, somewhat surprisingly, that the melittin/lipid mixing ratio needed to induce obvious morphological changes in the cholesterol-supplemented systems was lower than that in the pure PC systems (compare, e.g., Figs. 6 *B* and 8 *B*). As a consequence, structural alterations were observed in the cholesterol-containing liposome samples even at R_{eff} values considerably lower than those required to achieve maximum leakage within 15 min (Table 1). For instance, when melittin was added to DOPC/cholesterol liposomes at a concentration corresponding to $R_{eff} = 0.88 \times 10^{-3}$, a variety of new structures appeared in the samples. As seen in Fig. 8 *B*, the sample contained many seemingly unperturbed liposomes, but also some fused and ruptured structures, as well as a population of small closed liposomes of a size not seen in the melittin-free system. From Fig. 5, it is clear that despite the significant structural alterations revealed by cryo-TEM, only very modest leakage takes place at this low R_{eff}. Pronounced liposome aggregation and the formation of large bilayer sheets was detected when the amount of membrane-associated melittin was increased to $R_{eff} = 2.6 \times 10^{-3}$ (Fig. 8 *C*). This result helps explain the enhanced light scattering observed at the corresponding R_{eff} in the turbidity measurements (Fig. 2). No large liposome clusters were, on the other hand, observed at $R_{eff} = 1.2 \times 10^{-2}$, and, as shown in Fig. 8 *D*, the large bilayer sheets were now replaced by small open bilayers. Some important structural changes occurred over time in the latter sample. After incubation for 24 h, most of the material was found to be in small micelle-like structures (Fig. 8 *E*).

Melittin caused similar structural effects in the DOPC/cholesterol and POPC/cholesterol systems. For the latter system, cryo-TEM again revealed ruptured and fused liposomes at R_{eff} values lower than those needed for complete leakage within 15 min (Fig. 9 *B*). Further, for high melittin concentrations, a time-dependent breakdown of the liposomes into small micelle-like structures was evident (Fig. 9, *D* and *E*). It is noteworthy that at intermediate melittin concentrations, we documented large clusters of rather small open bilayers in the POPC/cholesterol samples (Fig. 9 *C*).

DISCUSSION

Association behavior

As revealed by the isotherms in Fig. 1, membrane lipid composition has a strong effect on the melittin association

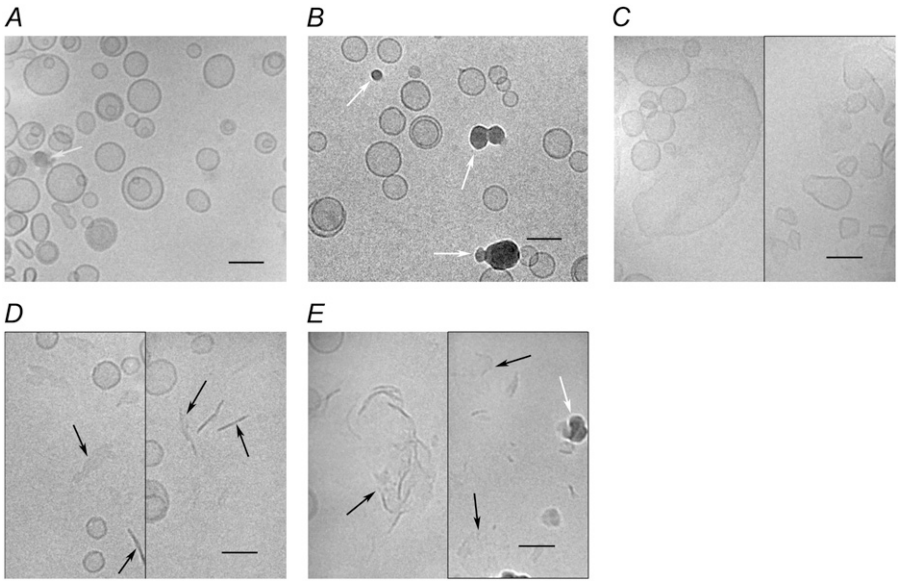

FIGURE 7 Aggregate structures as revealed by cryo-TEM before (*A*) and after (*B–E*) melittin addition to POPC liposomes. (*B*) Liposomes at $R_{eff} = 1.5 \times 10^{-3}$ ($R_i = 1.8 \times 10^{-3}$). (*C* and *D*) Examples of structures found at $R_{eff} = 7.2 \times 10^{-3}$ (*C*) and 3.2×10^{-2} (*D*) ($R_i = 7.5 \times 10^{-3}$ and 6.0×10^{-2}, respectively). (*E*) The structures found in sample *D* shown 72 h after melittin addition. Black arrows point to discrete open bilayer structures positioned either face- or edge-on; white arrows indicate ice crystals. Scale bar, 100 nm.

behavior. Analysis of the partition data using Eqs. 1 and 2 suggests that the difference between melittin's interactions with the various lipid membranes is expressed in the fitting parameter for the activity, *w*, rather than the partition coefficient K_P (Table 1). Thus, K_P varies only slightly between the different compositions, whereas *w* covers a wide range, from 24 for DOPC to 3.7×10^3 for POPC/cholesterol. In the expression used to fit the experimental association isotherms, all properties that may cause deviation from ideal partitioning, such as electrostatic interactions between peptides and inherent membrane properties, were put together into one simple activity parameter, *w* (Eq. 2). The use of this simple expression for the activity might look like taking a step backward compared to the theories put forward by Schwarz and Beschiaschvili (34), and thereafter expanded by Stankowski (35), and Kuchinka and Seelig (36). These theories use a Gouy-Chapman (G-C) approach to account for the nonideal melittin partitioning behavior. It is important to note that this approach relies on the assumption that the primary reason for the curved association isotherms is the electrostatic repulsions between the charged melittin molecules. Using the G-C approach, it has been established that the effective charge, z_P, of the peptide in its membrane-bound state is $\sim +2$ (12,34,36). This is considerably lower than the maximum possible charge of $+6$ for a free melittin molecule in water, and it has been argued that this discrepancy is partly

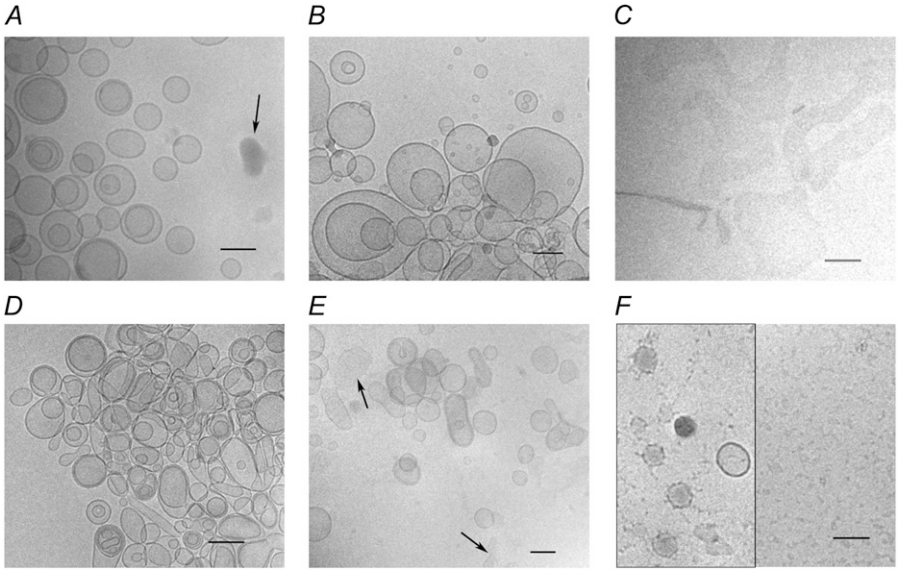

FIGURE 8 Aggregate structures as revealed by cryo-TEM before (*A*) and after (*B–F*) melittin addition to DOPC/cholesterol 60:40 liposomes. (*B*) Liposomes at $R_{eff} = 0.88 \times 10^{-3}$ ($R_i = 0.90 \times 10^{-3}$). (*C* and *D*) Sample structures found at $R_{eff} = 2.6 \times 10^{-3}$ ($R_i = 2.8 \times 10^{-3}$). (*E*) Structures found at $R_{eff} = 1.2 \times 10^{-2}$ ($R_i = 2.7 \times 10^{-2}$) immediately after melittin addition (*left*) and *F* shows the same sample after 24 h. Black arrows indicate ice crystals. Scale bar, 100 nm.

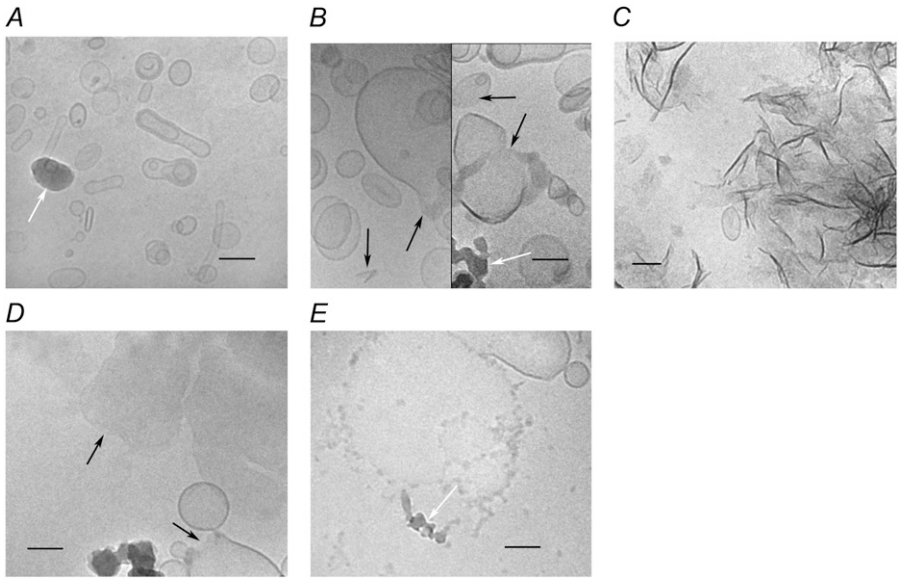

FIGURE 9 Aggregate structures as revealed by cryo-TEM before (*A*) and after (*B–E*) melittin addition to POPC/cholesterol 60:40 liposomes. (*B*) Liposomes at $R_{eff} = 0.53 \times 10^{-3}$ ($R_i = 0.67 \times 10^{-3}$). (*C* and *D*) Examples of structures found at $R_{eff} = 0.94 \times 10^{-3}$ ($R_i = 5.0 \times 10^{-3}$) and $R_{eff} = 1.1 \times 10^{-3}$ ($R_i = 2.7 \times 10^{-2}$) respectively). (*E*) The same sample as in *D* seen after 24 h. Black arrows point to discrete open bilayer structures, and white arrows indicate ice crystals. Scale bar, 100 nm.

due to the fact that with the G-C approach, melittin molecules are treated as point charges. This can be corrected for by employing a virial approach that also takes into account the excluded area in the membrane due to already bound melittin molecules (35). When we fit our binding data for melittin in the pure PC systems using the expression suggested by Schwarz and Beschiaschvili (31), we obtain values of z_P that correspond to 1.7 and 2.1 for DOPC and POPC, respectively. These values lie well in the range of those reported previously (12,34,36). However, if we use the same expression for the DOPC/cholesterol and POPC/cholesterol systems, we arrive at z_P values corresponding to 5.5 and 20, respectively. The unrealistically high z_P values, for the POPC/cholesterol case in particular, imply that nonelectrostatic contributions to the activity become relatively more important when the membrane is supplemented with cholesterol. Therefore, it appears reasonable to include changes, e.g., in the micromechanical properties of the membrane, in the expression for the activity.

Two trends are immediately evident from a comparison of the association isotherms in Fig. 1. First, cholesterol decreases melittin association with the liposomes, and second, melittin shows a more pronounced association with DOPC- than with POPC-containing liposomes. It is well known that cholesterol has a condensing effect on phospholipid membranes (37). In terms of micromechanical properties, the interaction manifests itself as a significant increase in the area compressibility modulus, K_A (38,39). As discussed by, e.g., Wolfenden (40), the energy of transfer of a solute from the aqueous phase into a membrane includes the cost of creating a cavity in the membrane phase. Because this cost is directly proportional to K_A, it is plausible that a membrane-penetrating molecule such as melittin will have more difficulty associating with cholesterol-containing membranes. Moreover, nonelectrostatic contributions to the activity can be expected to become relatively more important for a condensed and highly ordered cholesterol-containing membrane.

Our finding that melittin is more prone to associate with DOPC liposomes than with POPC liposomes is in line with earlier observations made by Rex and Schwarz (12). Since data based on micropipette pressurization of giant liposomes suggest that the K_A for DOPC is somewhat higher than that for 1-stearoyl-2-oleoyl-*sn*-glycero-3-phosphocholine (SOPC) (41), and since it is unlikely that the K_A for POPC is significantly larger than that for the closely related SOPC, it appears that differences in membrane area compressibility cannot explain the weaker association of melittin to POPC compared to DOPC membranes. The dissimilar association behavior must thus originate from differences in some other inherent properties of the two PC membranes. In contrast to POPC, DOPC has a slightly negative spontaneous curvature (10), and it can be speculated that the lower spontaneous curvature has a favorable effect on the melittin association process. It is, however, not straightforward why lower spontaneous curvature would lead to stronger melittin association. Systematic studies focused on the peptide alamethicin in fact suggest that the association free energy for the peptide increases, rather than decreases, with decreasing lipid spontaneous curvature (42). It is possible that structural differences between membrane-associated alamethicin and melittin can explain the seemingly opposite trends observed for the two peptides. Nevertheless, further investigations are clearly needed to fully clarify the effect of spontaneous curvature on the association behavior of melittin.

Helix induction is believed to constitute an important part of the driving force for membrane association of small peptides. The formation of the ordered secondary structure reduces the otherwise high energy cost of partitioning the peptide bonds in unfolded peptides (43). The difference in

melittin α-helical content observed between the pure DOPC and POPC systems (Fig. 4) is thus in line with the trend revealed by comparing the association isotherms (Fig. 1). A lower possibility for helix formation could theoretically also partly explain why cholesterol reduces the tendency for melittin to associate with the membranes. In line with this reasoning, the helical content was found to be considerably lower in the POPC/cholesterol than in the pure POPC system. Data retrieved by CD measurements for the DOPC-based systems suggest, on the other hand, only a marginal reduction in the melittin α-helical content upon addition of cholesterol. As mentioned in Results, CD measurements for the cholesterol-supplemented samples were performed under conditions where melittin, according to our cryo-TEM investigations, causes severe structural perturbations of the liposomes. The heterogeneous aggregate structure, including open membranes and possibly also nonbilayer structures, raises questions about potential component segregation. We therefore refrain from drawing any detailed conclusions from the CD data obtained in the DOPC/cholesterol and POPC/cholesterol systems. However, it is, noteworthy that the CD data, in line with the association isotherms in Fig. 1, indicate a more pronounced effect of cholesterol in the POPC compared to the DOPC system.

Correlating leakage and adsorption

Combining the results from the leakage and adsorption studies reveals two interesting features. First, by relating the leakage to the actual amount of melittin associated with the membranes, i.e., R_{eff}, it can be concluded that the ability of DOPC liposomes to resist melittin-induced leakage is greater than that of POPC liposomes. As shown in Table 1, this holds true regardless of whether the liposomes contain cholesterol or not. Second, the results show that once melittin has associated with the membrane, cholesterol does not offer any protection against leakage. Comparison of the results obtained for the POPC and POPC/cholesterol systems in fact suggest that the membranes become more sensitive to leakage in the presence of the sterol. It should be noted, however, that if the overall melittin concentration, rather than the membrane-bound fraction, is considered, our results support the common notion that cholesterol inhibits the bilayer lytic effect of melittin (3,10,14,15). In agreement with the results of this investigation, a number of previous studies (12,44,45) have reported that DOPC membranes are more resistant than POPC membranes to melittin-induced leakage. Further, Allende et al. found that melittin-induced leakage from SOPC was greater than from DOPC liposomes under the same experimental conditions (10). In the latter report, it is argued that lipid spontaneous curvature has an important influence on melittin's tendency to induce leakage, and that a negative spontaneous curvature hampers melittin-induced leakage. DOPC has a spontaneous curvature, $1/R_0$, of –0.011, whereas SOPC, similar to POPC, is estimated to have zero spontaneous curvature (10). The correlation between spontaneous curvature and the ability of antibacterial peptides to perturb lipid membranes has been addressed also for several other peptides (46–48). Based on the results of these studies, it has been suggested that upon adsorbing to the membrane surface, the peptides induce a positive curvature strain on the membrane. To relax the strain, the membrane has to bend and a toroidal-type pore is formed. The spontaneous curvature of the lipid, or lipid mixture, is believed to influence the number of adsorbed peptides needed to permeabilize the membranes. In line with this reasoning, a study by Lee et al. (49) shows that melittin starts to reorient from a parallel to a perpendicular orientation with respect to the bilayer when a critical, and lipid-composition-dependent, amount of melittin has adsorbed. The critical amount decreases with increasing spontaneous curvature of the lipid mixture. Our observation that more melittin needs to be associated with DOPC than with POPC liposomes to achieve comparable leakage is thus in qualitative agreement with the results from the reports cited above. However, if a universal relation between lipid spontaneous curvature and melittin-induced leakage should exist, it is expected that inclusion of cholesterol, which has negative spontaneous curvature ((50) and references therein), would increase the resistance of the liposomes to melittin-induced leakage. According to the results presented in Table 1, this is clearly not the case. It has been suggested that membrane area compressibility, in addition to spontaneous curvature, influences the extent of leakage caused by melittin. Data compiled by Allende et al. support a correlation between leakage and the compressibility modulus, K_{A}, so that the higher the K_{A}, the less leakage is induced by a certain amount of melittin (10). Since K_{A} is most likely somewhat higher for DOPC than for POPC, leakage data for the cholesterol-free systems (Table 1) agree with the expected trend. Our data obtained for the cholesterol-supplemented systems, on the other hand, are not consistent with the assumption of a straightforward and universal correlation between membrane area compressibility and leakage. More specifically, the presence of cholesterol tends to significantly increase K_{A} (36), but an equal or even lower amount of membrane-associated melittin is needed to achieve maximum leakage from the cholesterol-supplemented PC liposomes compared to the pure ones (Table 1).

In this context, it should be noted that under conditions corresponding to low R_{i} values, Allende et al. (10) observed reduced leakage from cholesterol-supplemented liposomes. However, the liposomes in the Allende et al. study were supplemented with 15 mol % phosphatidylserine to compensate for the low binding of melittin. The presence of this negatively charged lipid complicates a direct comparison with the results of the investigation described here. As shown by Strömstedt et al. (22), although melittin binds more avidly to liposomes with a net negative charge than to zwitterionic cholesterol-containing liposomes, less leakage is induced in the former case at similar R_{eff}. This fact, which has been ex-

plained in terms of an electrostatic arrest of melittin at the membrane surface (22), may help explain the comparably low leakage observed by Allende et al. (10). It is important to note that our observation that cholesterol fails to protect against leakage does not necessarily speak against the hypothesis that lipid spontaneous curvature and/or membrane area compressibility are of major relevance for the ability of melittin to permeabilize lipid membranes. As we discuss later, a more likely explanation is that the mechanism by which melittin induces leakage from cholesterol-supplemented liposomes is different from the corresponding mechanism in liposomes that contain PC only.

Changes in membrane morphology

The effect of melittin on lipid bilayer morphology has been studied for pure saturated phospholipids and also for mixtures of saturated phospholipids and cholesterol (14,16, 17,19,21,51). In a previous study, we employed cryo-TEM to visualize the effects of melittin interaction with DOPC/cholesterol liposomes and to explore the structural effects caused by inclusion of negatively charged lipids in the membrane (22). To our knowledge, no detailed structural investigations have been performed on pure DOPC, POPC, or POPC/cholesterol systems.

The systems without cholesterol

Previous freeze-fracture EM studies suggest that multilamellar liposomes composed of dipalmitoyldiphosphatidylcholine (DPPC) transform into unilamellar liposomes upon incubation with melittin at temperatures above the gel-to-liquid-crystalline phase transition temperature, T_m (18). When the temperature is reduced below the T_m, the liposomes transform into disclike structures with a diameter of 20–40 nm (16). If the temperature is then returned to above the T_m, the discs tend to fuse into extended bilayers (17,18). It has been suggested that the gel-phase discs represent nonlamellar structures or, alternatively, lamellar structures with a size too small to give the powder pattern expected for bilayers in ^{31}P-NMR measurements (21). The same sequence of structural transformations has also been reported for melittin-containing dimyristoyldiphosphatidylcholine systems (19). However, in the studies mentioned (16–19,21) there is a disagreement concerning whether disc formation can occur also above the T_m, i.e., in the liquid-crystalline phase. The cryo-TEM results obtained for cholesterol-free DOPC and POPC systems in this study show that at 25°C, i.e., well above the T_ms for these lipids, melittin induces formation of open lamellar structures. As seen in Fig. 7, *D* and *E*, these structures sometimes adopt a fairly small size and roughly circular shape. As mentioned earlier, the melittin-lipid mixtures were not structurally homogenous. Even at the highest R_i and R_{eff} values investigated, open and closed bilayers were observed to coexist in the DOPC and POPC systems. The open structures found in the POPC system were still present >72 h after mixing (Fig. 7 *E*), and it can thus be inferred that melittin not only induces, but also stabilizes, these structures, likely by aggregating at the bilayer edges. A similar structure has been suggested for discs formed in the DPPC/melittin system at a temperature below the T_m (16).

The structural information revealed by the cryo-TEM investigation may have important implications for the analysis and interpretation of data collected by other techniques. Results of this study show, for instance, that melittin promotes the formation of open membrane structures at peptide/lipid ratios considerably lower than commonly assumed. In this context, it is interesting to note that several previous studies carried out to verify, and determine the size of, melittin-induced toroidal pores in POPC membranes employed peptide/lipid mixing ratios corresponding to R_{eff} values close to or above 0.0072 (11,52). As is evident from the micrographs in Fig. 7, *B–D*, the presence of large membrane holes and open bilayer structures may under these circumstances confuse the interpretation of data.

The systems with cholesterol

Pott and Dufourc (21), as well as Monette et al. (51), show that the interaction of melittin with DPPC membranes is modified by inclusion of 30 mol % cholesterol. Isotropic NMR results, indicative of small discs or micelles, were observed at high mixing ratios. The presence of micelle-sized objects at high melittin/lipid ratios is consistent with our findings in the DOPC/cholesterol and POPC/cholesterol systems. Cryo-TEM revealed, however, that open and perturbed structures also occur at comparatively low melittin/lipid ratios. It is interesting to note that perturbed and open structures are formed at lower R_{eff} and R_i in the cholesterol-supplemented systems than in the pure DOPC and POPC systems. Thus, our findings show that cholesterol does not protect the liposomes from being ruptured. Another interesting observation in this context is that the type of structures present at high R_{eff} change with time. Thus, the sample images collected immediately after mixing show large bilayer flakes and a pronounced tendency for liposome aggregation (Figs. 8 and 9). This pronounced aggregation is supported by the observed turbidity measurements (Fig. 2). On the other hand, cryo-TEM images obtained from the same samples 24 h later display very small micelle-like structures coexisting with open bilayers and closed liposomes. Close inspection of Fig. 9 *E* suggests that the small structures bud off from the open bilayers. The time-dependent degradation of the bilayers into micelle-like structures explains why the turbidity of the POPC-cholesterol sample drops after 24 h. The reduced turbidity seen for the DOPC/cholesterol system only a short time after mixing with melittin to an R_{eff} of 1.2×10^{-2}, i.e., $R_i = 3.6 \times 10^{-2}$ (Fig. 2), probably reflects the decreased aggregation that was seen from cryo-TEM rather than immediate formation of the small micelle-like structures.

Correlating the effect of cholesterol on leakage with the changes in membrane morphology

A comparison of the R_{eff} values at which maximum leakage and liposome rupture occur reveals some important differences between the cholesterol-containing and cholesterol-free systems. In the case of pure POPC and DOPC liposomes, complete leakage was observed at R_{eff} values well below those needed to cause rupture or other large-scale changes in membrane morphology. Thus, the leakage in these systems took place from seemingly intact and structurally unperturbed liposomes. In contrast, for cholesterol-supplemented liposomes, major structural changes were observed at R_{eff} values lower than those needed to cause maximum leakage. As pointed out earlier, ruptured and intact liposomes were found to coexist in all the samples investigated. Since ruptured liposomes inevitably release their contents, a mechanism based on the formation of small, well defined pores is clearly insufficient to satisfactory explain the melittin-induced leakage recorded from our cholesterol-containing liposomes. The fact that cholesterol-supplemented DOPC liposomes fail to release more than ~70% of the entrapped CF molecules upon melittin addition (Fig. 5) further speaks against a leakage mechanism based on the formation of distinct pores. As discussed by, e.g., Andersson et al. (53), once membrane pores have been established, the net flow of probe molecules will continue until the concentration inside the liposomes is equal to that in the outside medium, i.e., a situation corresponding to 100% leakage. Results of the investigation described here thus support studies by Raghuraman and Chattopadhyay (3,54), which suggest that mechanisms other than pore formation might be responsible for melittin-induced leakage from erythrocytes and also from DOPC liposomes supplemented with 40 mol % cholesterol. It is worth noting, in this context, that the presence of 1,2-dioleoyl-*sn*-glycero-3-phosphoethanolamine, which, like cholesterol, tends to induce negative membrane curvature, appears to alter the mechanism for melittin-induced leakage from DOPC liposomes. Results recently published by van den Bogaart et al. suggest that although melittin-induced leakage from pure DOPC liposomes occurs via well defined pores, DOPC liposomes supplemented with 50 mol % DOPE release their contents due to a nonspecific process involving melittin-induced fusion or aggregation of the liposomes (9).

The polydisperse aggregate structures, and the significant morphological changes revealed by cryo-TEM over time, indicate an initially uneven distribution of melittin in the cholesterol-containing samples. It is plausible that melittin associates less with the membranes of intact liposomes than with the open-membrane structures. If melittin has a high affinity for curved surfaces, as suggested by its avid adsorption to spherical lysophosphatidylcholine micelles (55), it can be speculated that it preferentially adsorbs to the hemispherical edges of open-membrane structures. In this case, the membranes of the intact liposomes may contain only very small amounts of melittin. This might explain the inability of DOPC/cholesterol liposomes to release more than 70% of the entrapped CF during the course of the leakage experiments.

CONCLUSIONS

Experimentally determined association isotherms, as well as ellipsometry data, obtained in this study confirm that cholesterol reduces the association of melittin with DOPC and POPC membranes. Leakage measurements performed under conditions corresponding to equal peptide/lipid ratios in the membranes (equal R_{eff}) indicate equal or higher leakage rates in the cholesterol-supplemented systems. Thus, once melittin has associated with the membranes, cholesterol does not offer any protection against leakage. Systematic cryo-TEM investigations show that at sufficiently high concentrations, melittin causes liposome rupture and major structural rearrangements in all the investigated systems. It is worthy of note that the liposome breakdown appears to begin at lower peptide/lipid mixing ratios (R_i) in the cholesterol-supplemented systems. Comparison of leakage and cryo-TEM data suggests that melittin permeabilizes the lipid membrane via different mechanisms in the absence and presence of cholesterol. In the absence of cholesterol, leakage takes place in a manner compatible with the presence of small melittin-induced toroidal pores. In the presence of physiologically relevant concentrations of cholesterol, on the other hand, leakage is accompanied by major structural transformation of the liposomes. The increased bending rigidity mediated by cholesterol thus appears to hamper the formation of small distinct pores, and in this case adsorption of the peptide causes complete membrane disruption and formation of open-bilayer structures.

Financial support from the Swedish Research Council, the Swedish Foundation for Strategic Research, and the Knut and Alice Wallenberg Foundation is gratefully acknowledged.

REFERENCES

1. Raghuraman, H., and A. Chattopadhyay. 2006. Melittin: a membrane-active peptide with diverse functions. *Biosci. Rep.* 27:189–223.
2. Dempsey, C. E. 1990. The actions of melittin on membranes. *Biochim. Biophys. Acta.* 1031:143–161.
3. Raghuraman, H., and A. Chattopadhyay. 2005. Cholesterol inhibits the lytic activity of melittin in erythrocytes. *Chem. Phys. Lipids.* 134:183–189.
4. Bechinger, B., and K. Lohner. 2006. Detergent-like actions of linear amphipathic cationic antimicrobial peptides. *Biochim. Biophys. Acta.* 1758:1529–1539.
5. Brogden, K. A. 2005. Antimicrobial peptides: pore formers or metabolic inhibitors in bacteria? *Nat. Rev. Microbiol.* 3:238–250.
6. Wilcox, W., and D. Eisenberg. 1992. Thermodynamics of melittin tetramerization determined by circular dichroism and implications for protein folding. *Protein Sci.* 1:641–653.
7. Raghuraman, H., and A. Chattopadhyay. 2006. Effect of ionic strength on folding and aggregation of the hemolytic peptide melittin in solution. *Biopolymers.* 83:111–121.

8. Benachir, T., and M. Lafleur. 1995. Study of vesicle leakage induced by melittin. *Biochim. Biophys. Acta.* 1235:452–460.
9. van den Bogaart, G., J. T. Mika, V. Krasnikov, and B. Poolman. 2007. The lipid dependence of melittin action investigated by dual-color fluorescence burst analysis. *Biophys. J.* 93:154–163.
10. Allende, D., S. A. Simon, and T. J. McIntosh. 2005. Melittin-induced bilayer leakage depends on lipid material properties: evidence for toroidal pores. *Biophys. J.* 88:1828–1837.
11. Ladokhin, A. S., M. E. Selsted, and S. H. White. 1997. Sizing membrane pores in lipid vesicles by leakage of co-encapsulated markers: pore formation by melittin. *Biophys. J.* 72:1762–1766.
12. Rex, S., and G. Schwarz. 1998. Quantitative studies on the melittin-induced leakage mechanism of lipid vesicles. *Biochemistry.* 37:2336–2345.
13. Sato, H., and J. B. Feix. 2006. Peptide-membrane interactions and mechanisms of membrane destruction by amphipathic α-helical antimicrobial peptides. *Biochim. Biophys. Acta.* 1758:1245–1256.
14. Benachir, T., M. Monette, J. Grenier, and M. Lafleur. 1997. Melittin-induced leakage from phosphatidylcholine vesicles is modulated by cholesterol: a property used for membrane targeting. *Eur. Biophys. J. Biophys. Lett.* 25:201–210.
15. Raghuraman, H., and A. Chattopadhyay. 2004. Interaction of melittin with membrane cholesterol: a fluorescence approach. *Biophys. J.* 87: 2419–2432.
16. Dufourcq, J., J. F. Faucon, G. Fourche, J. L. Dasseux, M. Le Maire, and T. Gulik-Krzywicki. 1986. Morphological changes of phosphatidylcholine bilayers induced by melittin: vesicularization, fusion, discoidal particles. *Biochim. Biophys. Acta.* 859:33–48.
17. Dufourc, E. J., I. C. Smith, and J. Dufourcq. 1986. Molecular details of melittin-induced lysis of phospholipid membranes as revealed by deuterium and phosphorus NMR. *Biochemistry.* 25:6448–6455.
18. Dufourc, E. J., J. F. Faucon, G. Fourche, J. Dufourcq, T. Gulikkrzywicki, and M. Lemaire. 1986. Reversible disk-to-vesicle transition of melittin-DPPC complexes triggered by the phospholipid acyl chain melting. *FEBS Lett.* 201:205–209.
19. Dempsey, C. E., and B. Sternberg. 1991. Reversible disc-micellization of dimyristoylphosphatidylcholine bilayers induced by melittin and [Ala-14]melittin. *Biochim. Biophys. Acta.* 1061:175–184.
20. Monette, M., and M. Lafleur. 1996. Influence of lipid chain unsaturation on melittin-induced micellization. *Biophys. J.* 70:2195–2202.
21. Pott, T., and E. J. Dufourc. 1995. Action of melittin on the DPPC-cholesterol liquid-ordered phase: a solid state 2H-and 31P-NMR study. *Biophys. J.* 68:965–977.
22. Stromstedt, A. A., P. Wessman, L. Ringstad, K. Edwards, and M. Malmsten. 2007. Effect of lipid headgroup composition on the interaction between melittin and lipid bilayers. *J. Colloid Interface Sci.* 311:59–69.
23. Tenchov, B. G., R. C. MacDonald, and D. P. Siegel. 2006. Cubic phases in phosphatidylcholine-cholesterol mixtures: cholesterol as membrane ''fusogen''. *Biophys. J.* 91:2508–2516.
24. Klosgen, B., and W. Helfrich. 1997. Cryo-transmission electron microscopy of a superstructure of fluid dioleoylphosphatidylcholine (DOPC) membranes. *Biophys. J.* 73:3016–3029.
25. Lakowicz, J. R. 1999. Principles of fluorescence spectroscopy. Kluwer Academic/Plenum, New York London.
26. Perez-Paya, E., I. Porcar, C. M. Gomez, J. Pedros, A. Campos, and C. Abad. 1997. Binding of basic amphipathic peptides to neutral phospholipid membranes: a thermodynamic study applied to dansyl-labeled melittin and substance P analogues. *Biopolymers.* 42:169–181.
27. De Feijter, J. A., J. Benjamins, and F. A. Veer. 1978. Ellipsometry as a tool to study the adsorption behavior of synthetic and biopolymers at the air-water interface. *Biopolymers.* 17:1759–1772.
28. Vacklin, H. P., F. Tiberg, and R. K. Thomas. 2005. Formation of supported phospholipid bilayers via co-adsorption with beta-D-dodecyl maltoside. *Biochim. Biophys. Acta.* 1668:17–24.
29. Tiberg, F., I. Harwigsson, and M. Malmsten. 2000. Formation of model lipid bilayers at the silica-water interface by co-adsorption with non-ionic dodecyl maltoside surfactant. *Eur. Biophys. J.* 29:196–203.
30. Almgren, M., K. Edwards, and G. Karlsson. 2000. Cryo transmission electron microscopy of liposomes and related structures. *Colloids Surf. A. Physicochem. Eng. Asp.* 174:3–21.
31. Greenfield, N., and G. D. Fasman. 1969. Computed circular dichroism spectra for the evaluation of protein conformation. *Biochemistry.* 8: 4108–4116.
32. Sjogren, H., and S. Ulvenlund. 2005. Comparison of the helix-coil transition of a titrating polypeptide in aqueous solutions and at the air-water interface. *Biophys. Chem.* 116:11–21.
33. Constantinescu, I., and M. Lafleur. 2004. Influence of the lipid composition on the kinetics of concerted insertion and folding of melittin in bilayers. *Biochim. Biophys. Acta.* 1667:26–37.
34. Schwarz, G., and G. Beschiaschvili. 1989. Thermodynamic and kinetic studies on the association of melittin with a phospholipid bilayer. *Biochim. Biophys. Acta.* 979:82–90.
35. Stankowski, S. 1991. Surface charging by large multivalent molecules. Extending the standard Gouy-Chapman treatment. *Biophys. J.* 60:341–351.
36. Kuchinka, E., and J. Seelig. 1989. Interaction of melittin with phosphatidylcholine membranes. Binding isotherm and lipid head-group conformation. *Biochemistry.* 28:4216–4221.
37. Mouritsen, O. G., and M. J. Zuckermann. 2004. What's so special about cholesterol? *Lipids.* 39:1101–1113.
38. Evans, E., and D. Needham. 1986. Giant vesicle bilayers composed of mixtures of lipids, cholesterol and polypeptides. Thermomechanical and (mutual) adherence properties. *Faraday Discuss. Chem. Soc.* 81:267–280.
39. Needham, D., and R. S. Nunn. 1990. Elastic deformation and failure of lipid bilayer membranes containing cholesterol. *Biophys. J.* 58:997–1009.
40. Wolfenden, R. 2007. Experimental measures of amino acid hydrophobicity and the topology of transmembrane and globular proteins. *J. Gen. Physiol.* 129:357–362.
41. Rawicz, W., K. C. Olbrich, T. McIntosh, D. Needham, and E. Evans. 2000. Effect of chain length and unsaturation on elasticity of lipid bilayers. *Biophys. J.* 79:328–339.
42. Lewis, J. R., and D. S. Cafiso. 1999. Correlation between the free energy of a channel-forming voltage-gated peptide and the spontaneous curvature of bilayer lipids. *Biochemistry.* 38:5932–5938.
43. Ladokhin, A. S., and S. H. White. 1999. Folding of amphipathic α-helices on membranes: energetics of helix formation by melittin. *J. Mol. Biol.* 285:1363–1369.
44. Rex, S. 1996. Pore formation induced by the peptide melittin in different lipid vesicle membranes. *Biophys. Chem.* 58:75–85.
45. Bhakoo, M., T. H. Birkbeck, and J. H. Freer. 1984. Phospholipid-dependant changes in membrane permeability induced by staphylococcus δ-lysin and bee venom melittin. *Can. J. Biochem. Cell Biol.* 63:1–6.
46. Zhao, H., R. Sood, A. Jutila, S. Bose, G. Fimland, J. Nissen-Meyer, and P. K. Kinnunen. 2006. Interaction of the antimicrobial peptide pheromone Plantaricin A with model membranes: implications for a novel mechanism of action. *Biochim. Biophys. Acta.* 1758:1461–1474.
47. Hallock, K. J., D. K. Lee, and A. Ramamoorthy. 2003. MSI-78, an analogue of the magainin antimicrobial peptides, disrupts lipid bilayer structure via positive curvature strain. *Biophys. J.* 84:3052–3060.
48. Matsuzaki, K., K. Sugishita, N. Ishibe, M. Ueha, S. Nakata, K. Miyajima, and R. M. Epand. 1998. Relationship of membrane curvature to the formation of pores by magainin 2. *Biochemistry.* 37:11856–11863.
49. Lee, M. T., W. C. Hung, F. Y. Chen, and H. W. Huang. 2005. Many-body effect of antimicrobial peptides: on the correlation between lipid's spontaneous curvature and pore formation. *Biophys. J.* 89:4006–4016.

50. Karatekin, E., O. Sandre, H. Guitouni, N. Borghi, P. H. Puech, and F. Brochard-Wyart. 2003. Cascades of transient pores in giant vesicles: line tension and transport. *Biophys. J.* 84:1734–1749.

51. Monette, M., M. R. Van Calsteren, and M. Lafleur. 1993. Effect of cholesterol on the polymorphism of dipalmitoylphosphatidylcholine/melittin complexes: an NMR study. *Biochim. Biophys. Acta.* 1149:319–328.

52. Yang, L., T. A. Harroun, T. M. Weiss, L. Ding, and H. W. Huang. 2001. Barrel-stave model or toroidal model? A case study on melittin pores. *Biophys. J.* 81:1475–1485.

53. Andersson, A., J. Danielsson, A. Graslund, and L. Maler. 2007. Kinetic models for peptide-induced leakage from vesicles and cells. *Eur. Biophys. J. Biophys. Lett.* 36:621–635.

54. Raghuraman, H., and A. Chattopadhyay. 2007. Orientation and dynamics of melittin in membranes of varying composition utilizing NBD fluorescence. *Biophys. J.* 92:1271–1283.

55. Lundquist, A., P. Wessman, A. R. Rennie, and K. Edwards. 2008. Melittin-lipid interaction: a comparative study using liposomes, micelles and bilayerdisks. *Biochim. Biophys. Acta*. In press.